doi.org/10.1002/cbdv.202100365

FULL PAPER

CHEMISTRY & BIODIVERSITY

Biochemical Characterization, Phytotoxic Effect and Antimicrobial Activity against Some Phytopathogens of New Gemifloxacin Schiff Base Metal Complexes

Amira A. Mohamed,*[a] Hazem S. Elshafie,*[b] Sadeek A. Sadeek,*[c] and Ippolito Camele*[b]

[a] Department of Basic Science, Zagazig Higher Institute of Engineering and Technology, 44519 Zagazig, Egypt, e-mail: amira222283@yahoo.com; aa.adaim@science.zu.edu.eg

[b] School of Agricultural, Forestry, Food and Environmental Sciences, University of Basilicata, Viale dell'Ateneo Lucano 10, 85100 Potenza, Italy, e-mail: hazem.elshafie@unibas.it; ippolito.camele@unibas.it

[c] Department of Chemistry, Faculty of Science, Zagazig University, 44519 Zagazig, Egypt, e-mail: s_sadeek@zu.edu.eg

String of Fe(III), Cu(II), Zn(II) and Zr(IV) complexes were synthesized with tetradentateamino Schiff base ligand derived by condensation of ethylene diamine with gemifloxacin. The novel Schiff base (4*E*,4′*E*)-4,4′-(ethane-1,2-diyldiazanylylidene)bis{7-[(4*Z*)-3-(aminomethyl)-4-(methoxyimino)pyrrolidin-1-yl]-1-cyclopropyl-6-fluoro-1,4-dihydro-1,8-naphthyridine-3-carboxylic acid} (GMFX-en) and its metal complexes were identified and confirmed by elemental analyses, FT-IR, UV/VIS, ^{1}H-NMR spectra, magnetic susceptibility, conductometric measurements and thermal analyses. The FT-IR spectral data showed the chelation behavior of GMFX-en toward the metal ions through oxygen of carboxylate group and nitrogen of azomethine group. In the light of all spectral data, these complexes presumably have octahedral geometry configurations. Thermal analysis specified that the decaying of the metal complexes exist in two or three steps with the final residue metal oxides. Antimicrobial activity of the new prepared metal complexes was screened against some common phytopathogens and their mode of action has been also discussed. The potential phytotoxic effectiveness of the new complexes was furthermore inspected on two commonly experimental plants. The complexes showed significant antimicrobial and phytotoxic effects against the majority of tested phytopathogens and the two tested plants, respectively. The potential antimicrobial activity of the complexes proved their possibility to be used successfully in agropharmacutical industry to control many serious phytopathogens. The phytotoxicity of the studied complexes also indicated their possibility as potential bio-based herbicides alternatives to weed control in crop fields.

Keywords: gemifloxacin Schiff base, metal complexes, antimicrobial activity, phytotoxicity, chelation theory, phytopathogens.

Introduction

Schiff bases can be effortlessly produced by the intensification reaction of primary amines together with carbonyl compounds. Schiff base ligands have been substantially studied in coordination chemistry due to their ease of synthesis, effectively steric, electronic features, and good solubility in many solvents.[1,2] The presence of azomethine group in Schiff base ligands performs a paramount role in their antimicrobial activities. Schiff base ligand is capable of coordinating with metal ions and stabilize them in various oxidation state and increased their antimicrobial activity depending on dipole moment, solubility, their enzymatic action, and cell permeability.[3–5] Schiff base complexes have been utilized as model for biological procedures and as a catalytic for oxidation and polymerization of organic compounds.[6] Schiff

Supporting information for this article is available on the WWW under https://doi.org/10.1002/cbdv.202100365

base may be bi. di, tri or polydentate chelates together with metal ions through nitrogen and oxygen donor atoms formulation steady complexes.[7–13]

Gemifloxacin (GMFX) is an artificial wide ranging antimicrobial compound versus both Gram-positive and negative bacteria.[14] GMFX implicates an effective antibacterial activity against respiratory tract pathogens.[14] GMFX can be interrogated with aliphatic or aromatic amines supply a Schiff base.[14,15] In the literature, an attention has been paid to fluoroquinolones Schiff base complexes with transition metals.[16] On the other hand, the heavy metals and antibiotics could produce polluting molecules and induce phytotoxicity for crops. So, it is important to evaluate the phytotoxic effect of these new synthesized complexes for determining the possibility for their using in agropharmaceutical industry.[17]

In view of the above consideration, the goal of this study was to evaluate the impact of certain elements, such as Fe(III), Cu(II), Zn(II) and Zr(IV) on the efficiency of gemifloxacin in new form as GMFX-en (*Figure 1*). The compounds were investigated by elemental analysis, molar conductance measurements, FT-IR, UV/VIS, ^{1}H-NMR and thermal analyses. Whereas the antimicrobial activity was assessed towards phytopathogenic fungi: *Monilinia fructicola* (G. Winter) Honey, *Penicillium digitatum* (Pers.) Sacc., and *Colletotrichum acutatum* J.H. Simmonds and three bacterial species: *Clavibacter michiganensis* corrig. (Smith) Davis et al., *Xanthomonas campestris* Pammel (Dowson) and *Bacillus megaterium* (Pammel) Dowson. Phytotoxicity assay was performed against *Solanum lycopersicum* L. (tomato) and *Lepidium sativum* L. (cress).

Results and Discussion

The new prepared metal complexes of Fe(III), Cu(II), Zn(II) and Zr(IV) with GMFX-en are stable, colored, and non-hygroscopic in nature. The complexes were solvable in dimethylformamide and dimethyl sulfoxide. The exquisite physical features and distinctive data of the synthesized ligand and its metal complexes were measured (*Table 1*). The results of the chemical analysis showed that all the complexes were air stable at the room temperature. At room temperature, the molar conductance of GMFX-en in the free state is 17.50 $\Omega^{-1}\,mol^{-1}\,cm^2$, and the same data for metal complexes has been reported to range from 100.82 to 270.69 $\Omega^{-1}\,mol^{-1}\,cm^2$. Conductance statistics demonstrate that the metal complexes were electrolyte in contrast with GMFX-en.[16,18]

FT-IR Spectral Studies

Table 2 lists the positions of the significant FT-IR bands of Schiff base and its metal complexes. FT-IR of the complexes (*Figure S1*) is compared with those of GMFX-en orderly to mark the spot of assortment that possibly implicated in chelation. The GMFX-en spectrum revealed that the bands were obscured specialized for the bands of NH_2 group for ethylene diamine and C=O of pyridone group of GMFX. Registered a strong band at 1634 cm^{-1} refers to the C=N and it is determined to condensation of the amino group with a pyridone group, as a result of the formation of Schiff base linkage.[19] Complexes spectra involved bands expand from 3428–3433 cm^{-1} generated from the vibration of O–H signalizing the subsistence of water molecules in all complexes.[13] The influence of oxygen of carboxylate group with metal ions has been registered by the obscurity of the band at 1725 cm^{-1}

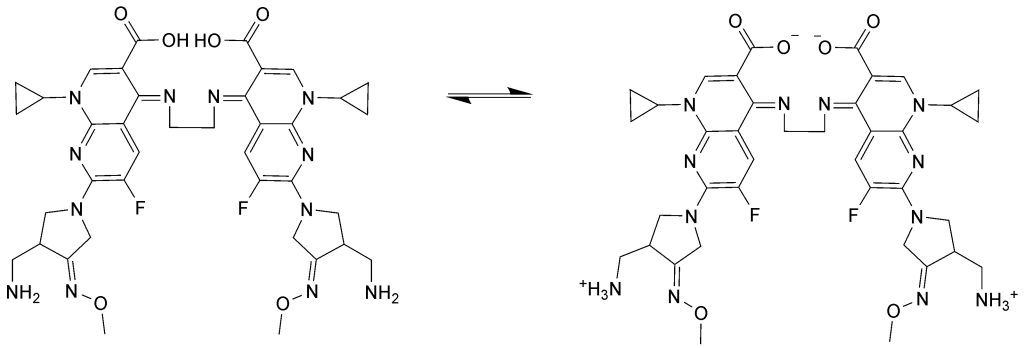

Figure 1. Structure of GMFX-en (4*E*,4′*E*)-4,4′-(ethane-1,2-diyldiazanylylidene)bis{7-[(4*Z*)-3-(aminomethyl)-4-(methoxyimino)pyrrolidin-1-yl]-1-cyclopropyl-6-fluoro-1,4-dihydro-1,8-naphthyridine-3-carboxylic acid}.

Table 1. Elemental analysis and physico-analytical data for GMFX-en and its metal complexes.

Compounds (M.F.)	M.Wt.	Yield%	M.p./°C	Color	Found (calc.) %					Λ Ω^{-1} mol^{-1} cm^2
					C	H	N	M	Cl	
GMFX-en ($C_{38}H_{44}F_2N_{12}O_6$)	802.762	81.00	340	Yellowish-white	56.70 (56.80)	5.40 (5.48)	20.80 (20.92)	–	–	17.50
Complex A ($FeC_{38}H_{62}F_2N_{12}O_{15}Cl_3$)	1127.107	77.20	300	Dark-red	40.31 (40.45)	5.42 (5.50)	14.72 (14.90)	4.89 (4.95)	9.36 (9.43)	270.69
Complex B ($CuC_{38}H_{54}F_2N_{12}O_{15}S$)	1052.218	80.10	220	Brown	41.80 (41.89)	5.25 (5.32)	15.36 (15.43)	5.72 (5.83)	–	100.82
Complex C ($ZnC_{38}H_{54}F_2N_{12}O_9Cl_2$)	1029.142	75.36	210	Light-brown	44.20 (44.31)	5.12 (5.24)	16.26 (16.32)	6.30 (6.35)	6.78 (6.88)	180.50
Complex D ($ZrC_{38}H_{56}F_2N_{12}O_{13}Cl_2$)	1088.886	72.69	300	Dark-brown	41.80 (41.87)	5.10 (5.14)	15.35 (15.42)	8.30 (8.37)	6.46 (6.51)	185.10

and presence of new band around 1635 cm^{-1} in the entire complexes spectra.[20] Subsistence of the asymmetric stretching vibration band in 1634–1636 cm^{-1} region and ν_{sym} in the region of 1356–1388 cm^{-1} with $\Delta\nu > 200$ cm^{-1} for the ligated carboxylate group indicated the carboxylate group mono dentate interacting through one of oxygen atoms.[13,21] Furthermore, the shift of the characteristic band of azomethine group from 1522 cm^{-1} to 1547 cm^{-1} in all certain complexes spectra specified participation of C=N group in interaction with metal ions. New bands in the regions 467–470 cm^{-1}and 420–432 cm^{-1}, matched to ν (M–O) and ν (M–N) vibration supporting the pointed out the mode of coordination (*Figure 2*).[22,23]

Electronic Spectra and Magnetic Studies

The assignments of the spotted electronic absorption bands of the GMFX-en and its metal complexes, magnetic data, and molar absorptivity (ϵ) of the established complexes are indexed in *Table 3*. Actually, the occurrences of diverse bands in the electronic spectra of GMFX-en display bands at 237, 268 and 345 nm (*Figure 3*) that may be referred to π-π* and n-π* transitions, respectively.[24–26] The electronic spectrum of the complex A exhibits an L→M (C.T) at 450 nm.[27] This complex presumably has octahedral configuration, and geometry is confirmed by measured magnetic moment (μ_{eff} = 1.80 B.M.).[28–30] For complex B electronic spectrum exhibits an L→M (C.T) charge transfer band at 480 nm.[31] The band detected at 580 nm for copper complex may be referred to $^2B_{1g} \rightarrow {}^2E_g$ transition.[32,33] The Cu(II) complex's magnetic moment (1.70 B.M.) is very similar to the spin value (1.73 B.M.) predicted for one unpaired electron, indicating an octahedral geometry. The electronic spectrum of complexes C and D exhibit an M→L (C.T) charge transfer bands at 445 and 424 nm. In the light of these results, these complexes presumably have octahedral configurations.[34,35]

^{1}H-NMR Spectra

The ^{1}H-NMR spectra of the ligand and its complexes were registered to emphasize the binding of the Schiff base to the metal ions (*Table S1*, *Figure 4*).[36,37] The complexes did not detect the signal at 11 ppm (COOH) in the GMFX-en spectrum, asserting that the ligand was deprotonated and chelated with metal ions.[38] Furthermore, owing to the existence of water molecules in the complexes, the ^{1}H-NMR spectra for

Table 2. Selected infrared absorption frequencies (cm^{-1}) for GMFX -en and its metal complexes.

Compounds	ν(O–H); H_2O; COOH	ν(C=O); COOH	$\nu_{as}(COO^-)$	ν(C=N)	$\nu_s(COO^-)$	ν (Zr=O)	ν(M–O), ν(M–N)
GMFX-en	3432mbr	1725s	–	1634vs	–	–	651w, 627w, 554w
Complex A	3433mbr	–	1634vs	1574m	1381w	–	640m, 562m, 535m
Complex B	3433sbr	–	1634vs	1522m	1388w	–	638w, 554w, 510m
Complex C	3428sbr	–	1636vs	1573m	1378w	–	636m, 560m, 538m
Complex D	3428sbr	–	1636vs	1531w	1356w	813m	639m, 559m

Key: s = strong, w = weak, m = medium, ν = stretching.

complexes indicate a novel peak in the range 4.20–4.55 ppm. Matching the GMFX-en Schiff base's key peaks to their complexes, The spectra of complexes with the chemical change induced by Schiff base binding to the metal ion contain all of the peaks of the free ligand.[39–41]

Thermal Analyses (TG and DTG) and Thermodynamic Parameters

The stoichiometry of the resultant volatile decaying components as well as the properties of the complexes was studied employing thermal analyses. The TG decay stages with the temperature maximum and weight loss for the complexes are indexed in *Table 4* and presented graphically in *Figure 5*. TG data for GMFX-en manifested one stage of decaying with temperature maxima 171, 338 and 532 °C corresponding to the loss of $18C_2H_2 + 2HF + 2NH_3 + 6NO + 2N_2$ with total weight loss amounted to 96.90% (calc. 97.02%). The TG curve of complex A exhibited two stages from 25 to 132 °C and 132 to 680 °C. The initial stage of decay, with a maximum temperature of 69 °C with a mass loss of 11.20% (calc. 11.18%) may be assigned to the removal of seven non- absorbed coordinated water molecules. The last step showed mass loss of 76.18% (calc. 76.41%), leaving the residue observed over 670 °C comparable to $0.5Fe_2O_3 + 5$ C related to the mass loss of 12.62% (calc. 12.41%). The thermogram of complex B showed three stages in the extent 25 to 137 °C, 137 to 211 °C and 211 to 650 °C. The first step due to the loss of $5H_2O$ lattice water with mass loses 8.64% (calc. 8.26%). The second step from 137 up to 211 °C display loss of 10 $C_2H_2 + 2H_2O$ species showed mass loss of 27.34% (calc. 27.19%). The last step showed $6C_2H_2 + CO + 2HF + H_2S + 4NO_2 + 2NH_3 + H_2$ species corresponding to 51.02% (calc. 51.73%) leaving at the back the residue observed over 998 °C analogous to CuO + 5 C related to mass loss of 13.00% (calc. 12.82%). The complex C with in the temperature range of 35 to 1000 °C, the complex started decomposition at 35 °C in three distinct degradation phases. Within the temperature range of 35 to 116 °C, the first step of decomposition corresponded to the loss of $3H_2O$ lattice water, resulting in a weight loss of 5.52%, which agrees well with the calculated value of 5.25%. The loss of Schiff base ligand molecules and coordinated water molecules were assigned to the second and third stages of decaying, which happened between 116 and 650 °C. It represented an 82.57% weight loss, which is in good agreement with the measured estimate of 83.35%, leaving at the back the

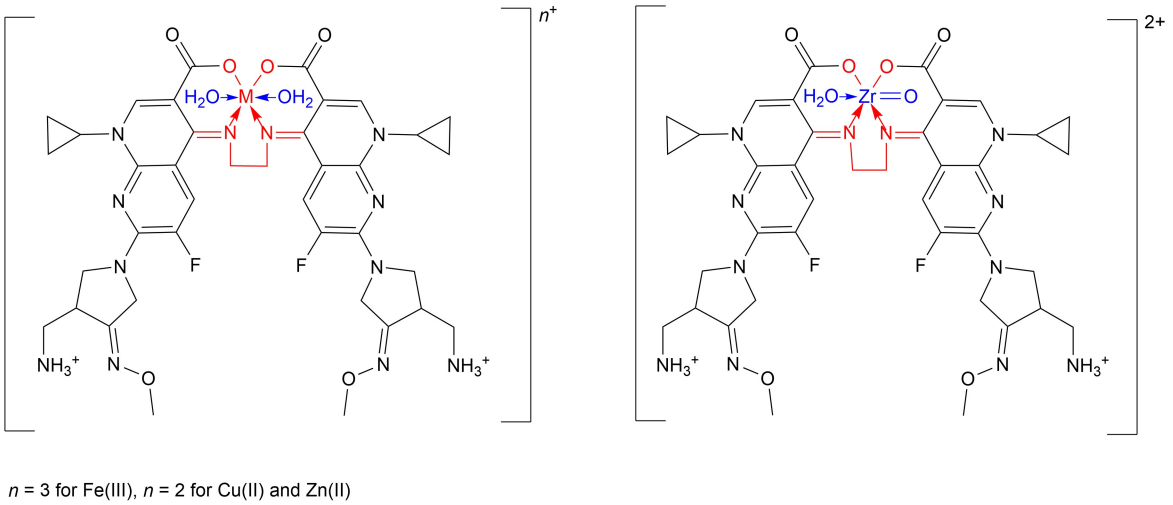

Figure 2. Structures of complexes A, B, C and D. Complex A: M = Fe(III), $n = 3$ ($FeC_{38}H_{62}F_2N_{12}O_{15}Cl_3$). Complex B: M = Cu(II), $n = 2$ ($CuC_{38}H_{54}F_2N_{12}O_{15}S$). Complex C: M = Zn(II), $n = 2$ ($ZnC_{38}H_{54}F_2N_{12}O_9Cl_2$). Complex D: M = Zr(IV), $n = 2$ ($ZrC_{38}H_{56}F_2N_{12}O_{13}Cl_2$).

residue observed over 999 °C analogous to ZnO + 3 C related to mass loss of 12.00% (calc. 11.40%). Lastly, the thermogram of complex D showed two steps in the range 31–125 °C and 125–660 °C. The first step due to loss of $5H_2O$ uncoordinated water molecules showed mass loss of 8.23% (calc. 8.26%). The second step showed loss of ligand molecules and coordinated water molecules corresponding to 76.77% (calc.76.01%), leaving at the back the residue observed over 660 °C analogous to $ZrO_2 + 4C$ related to mass loss of 15.00% (calc. 15.72%).

The kinetic factors such as (ΔH*), (E*), (G*), and (S*) (*Table 5*) were graphically tested using the Coats-Redfern and Horowitz-Metzger models equations (*Figure S2*).[42,43] Decomposition steps of activation energies were found to be in the range of 61.44–229.49 kJ mol1.[44,45] The positive sign of G* for complexes demonstrated that the final residue's free energy was higher than that of the initial compounds, implying that all decomposition steps were non-spontaneous. For the subsequent decomposition stages of a given complex, the values of the activation, ΔG*, increased significantly. This can be explained by the fact that substantially rising the values of TΔS* from one stage to the next overrides the values of ΔH*. Negative ΔS* values for the degradation process, on the other hand, suggested that the activated complex was more ordered than the reactants or that the reaction was sluggish.[46,47]

Antimicrobial Activity

Bactericidal Effect

The results of antibacterial activity of the compounds were represented in (*Figure 6*) where all tested treatments showed antibacterial effects against all tested bacteria especially at the higher tested concentrations. The highest antibacterial activity against *C. michiganensis* was spotted in the case of GMFX-en and complex B at 250 ppm (*Figure 4*). Regarding *B. megaterium* and *X. campestris* the highest substantial effect was observed in the case of GMFX-en at 250 ppm followed by the complex C at 250 ppm. On the other hand, complex D at 100 ppm showed the lowest effect against *B. megaterium* and the same complex did not show any effect against *X. campestris* (*Figure 6*).

Fungicidal Effect

GMFX-en and its complexes were verified for fungicidal activity versus three serious phytopathogenic fungi. (*P. digitatum*, *C. acutatum* and *M. fructicola*) compared to the positive control Azoxystrobin (*Table 6*). Results were demonstrated as fungal growth inhibition percentage. All examined substances clarified antifungal effect in a dose dependent manner. The best antifungal effect against *P. digitatum* was observed in the case of the complexes A and B at 100 ppm. On the other hand, the lowest effect was observed in the case of GMFX-en at 50 ppm compared to Azoxystrobin. The highest activity against *C. acutatum* was obtained in the case of Azoxystrobin followed

Table 3. UV/VIS spectra for GMFX-en and its metal complexes.

Compounds	μ_{eff}(B.M.)	π-π^* transitions λ_{max} (nm)	ν (cm^{-1})	ϵ (M^{-1} cm^{-1})	n-π^* transitions λ_{max} (nm)	ν (cm^{-1})	ϵ (M^{-1} cm^{-1})	Ligand-metal Charge transfer λ_{max} (nm)	ν (cm^{-1})	ϵ (M^{-1} cm^{-1})	d-d transition λ_{max} (nm)	ν (cm^{-1})	ϵ (M^{-1} cm^{-1})
GMFX-en	–	237	42194	2583	345	28985	944	–	–	–	–	–	–
		268	37313	2169									
Complex A	1.80	233	42918	898	343	29154	191	450	22222	188	534	18726	125
		265	37735	840									
Complex B	1.70	267	37453	1686	343	29154	645	480	20833	200	580	17241	100
Complex C	–	266	37593	1024	341	29325	281	445	22471	308	–	–	–
Complex D	–	239	41841	787	340	29411	125	424	23584	188	–	–	–

by complex C and GMFX-en at 100 ppm. The lowest effect was obtained with GMFX-en 50 ppm. There is no observed activity in the case of the complexes A and B at both tested doses and the complex B 50 ppm (*Table 6*). Furthermore, the complexes A, B, C and D at 100 ppm displayed the highest activity against *M. fructicola*. The lowest substantial effect has been observed in the case of GMFX-en 50 ppm.

Mode of Action

The obtained microbicide effect of the studied compounds might be due to the chemical structures of the free ligand as well as the toxicity of the studied metal ions.[48,49] The principle of cell permeability of the tested microorganisms clarified the enhanced antimicrobial activity of newly prepared metal chelates.[50–52] The polarity of metal ions can be reduced in particular by partially sharing the positive charge with the parent ligand's donor groups and as a result of orbital overlap with the ligand orbitals.[53] On the other hand, the chelation process enhancing the delocalization of electrons above the chelate ring, which increase the lipophilicity of the central ions. Because of the increase in lipophilicity, the tested compounds were able to penetrate deeper into the microorganism's cells.[54,55]

Phytotoxicity Effect

GMFX-en and its metal complexes were found to be extremely phytotoxic to all of the plants examined, *S. lycopersicum* and *L. sativum*, at all tested concentrations. In contrast to the control treatment, the studied compounds have decreased the seeds germination and radical elongation for both tested plants.

Conclusions

This study investigated the new trace metal complexes resulted from the interaction of some biological ions such as Fe(III), Cu(II) Zn(II) and Zr(IV) with GFFX-en which formed from the condensation reaction of GMFX with ethylene diamine. Results showed that the studied compounds have notable antimicrobial effect, in a dose-dependent manner, against all tested phytopathogens. The chemical structure of the free ligand GMFX-en and its toxic nature are both important factors in its promising antimicrobial activity of some trace elements. In addition, the examined compounds showed a significant phytotoxic effect on the two tested plants. The potential antimicrobial and

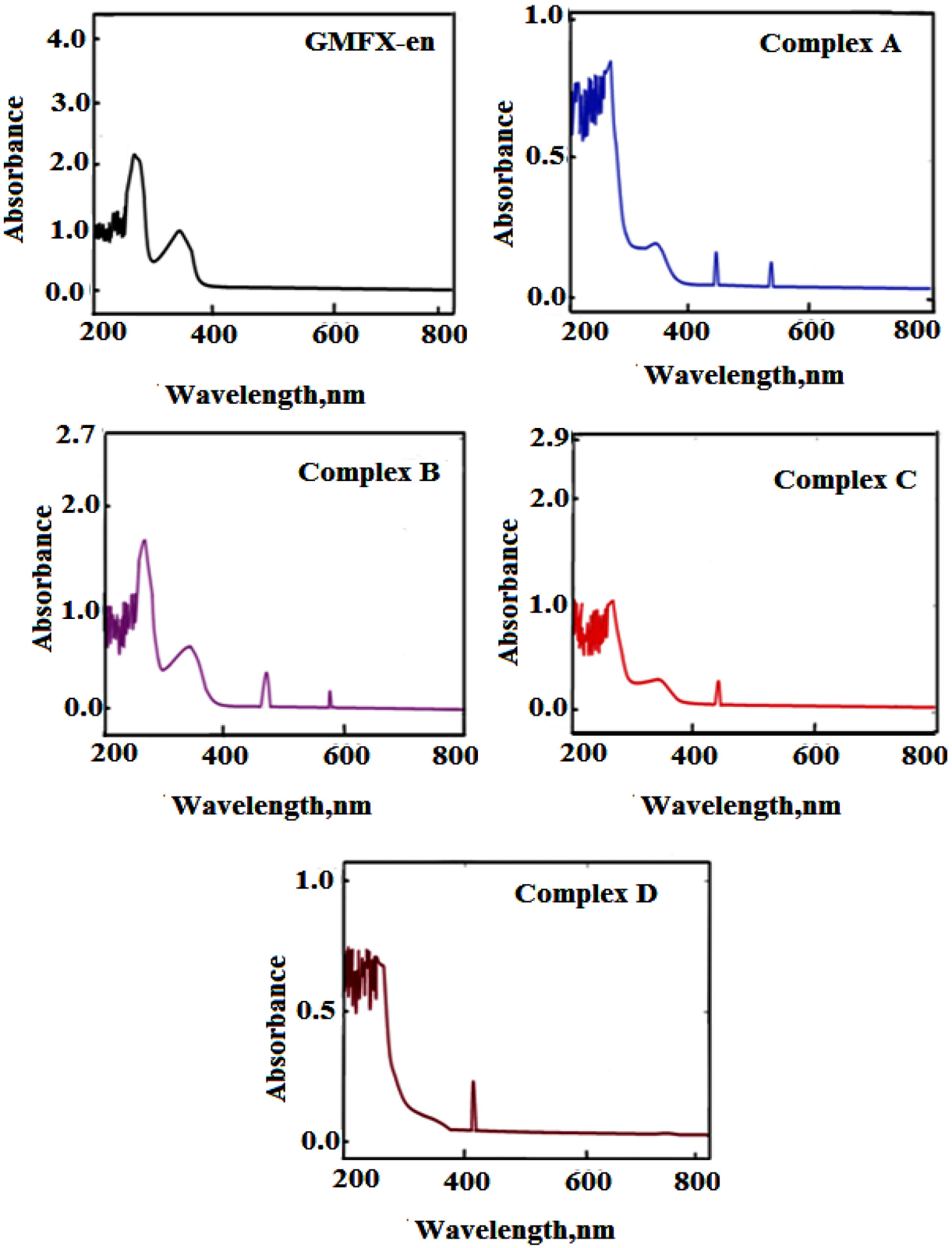

Figure 3. Electronic absorption spectra for GMFX-en and its metal complexes.

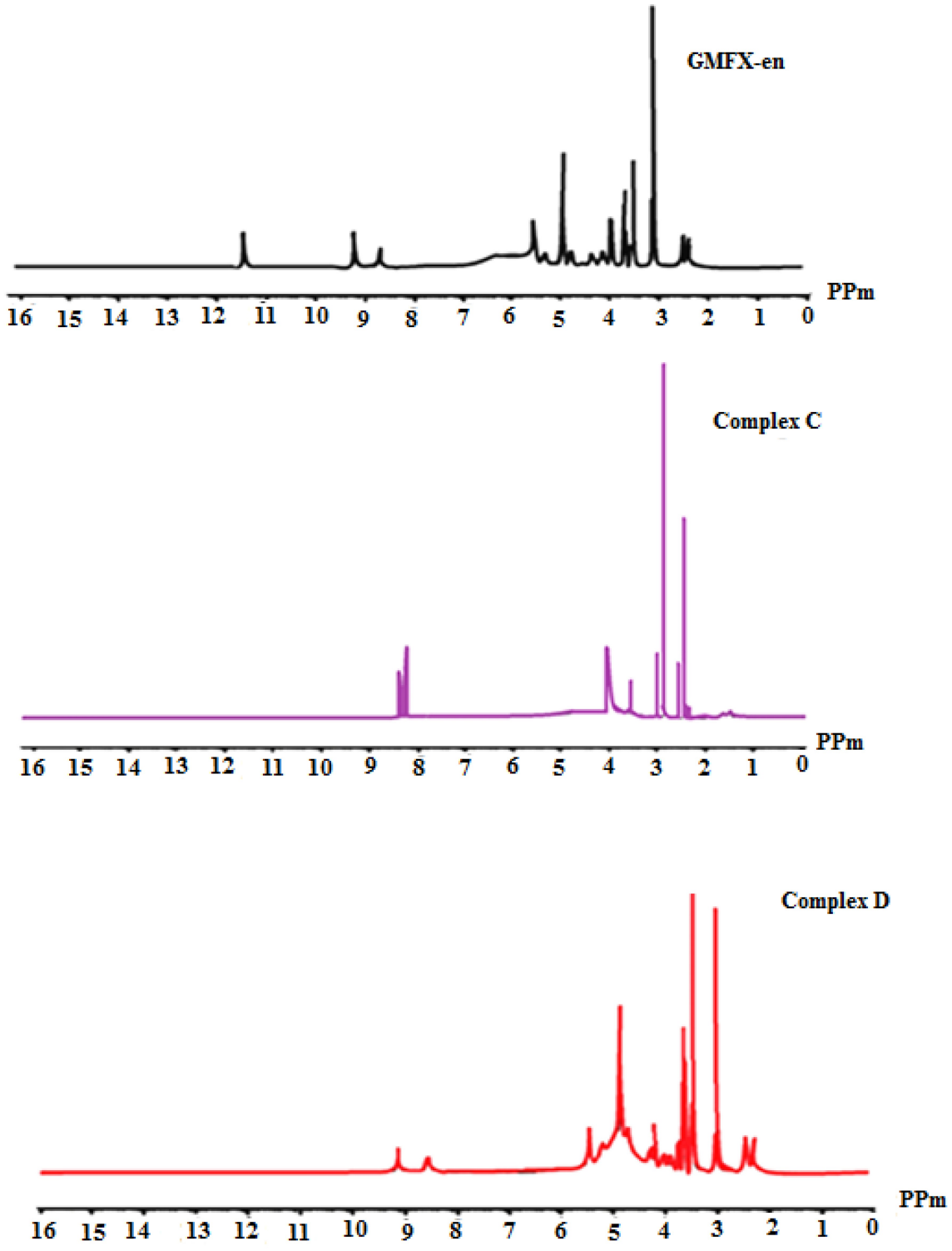

Figure 4. ^{1}H-NMR spectra for GMFX-en and its metal complexes.

Table 4. The maximum temperature T_{max} (°C) and weight loss values of the decomposition stages for GMFX-en and its metal complexes.

Compounds	Decomposition	T_{max} (°C)	Weight loss (%)		Lost species
			Calc.	Found	
GMFX-en	First step	172, 338, 532	96.90	97.02	$18C_2H_2+2HF+2NH_3+6NO+2N_2$
	Total loss		96.90	97.02	
	Residue		3.10	2.98	2C
Complex A	First step	69	11.18	11.20	$7H_2O$
	Second step	337	76.41	76.18	$16C_2H_2+2HF+CO+3HCl+2NH_3+5N_2+2.5H_2O$
	Total loss		87.59	87.38	
	Residue		12.41	12.62	$0.5Fe_2O_3+5C$
Complex B	First step	78	8.26	8.64	$5H_2O$
	Second step	183,269	27.19	27.34	$10C_2H_2+2H_2O$
	Third step	489	51.73	51.02	$6C_2H_2+CO+2HF+H_2S+4NO_2+2NH_3+H_2$
	Total loss		87.18	87.00	
	Residue		12.82	13.00	$CuO+5C$
Complex C	First step	93	5.25	5.52	$3H_2O$
	Second step	316	38.88	38.70	$14C_2H_2+2H_2O$
	Third step	472, 888	44.47	43.78	$2HF+2HCl+2NH_3+4\,N_2+2NO_2+CO$
	Total loss		88.60	88.00	
	Residue		11.40	12.00	$ZnO+3C$
Complex D	First step	78	8.26	8.23	$5H_2O$
	Second step	426	76.01	76.77	$17C_2H_2+2HF+2NH_3+2HCl+H_2O+2NO_2+4N_2$
	Total loss		84.28	85.00	
	Residue		15.72	15.00	ZrO_2+4C

phytotoxic effects of the new metal complexes indicated that they could be used effectively in controlling both serious phytopathogens and harmful weeds. In addition, the new innovative complexes could minimize the risk of appearance new resistant strains of fungal, bacterial, or harmful weeds to the traditional chemical compounds.

Experimental Section

Chemicals

Whole chemicals utilized were of analytical reagent grade and applied with no additional purifying. GMFX, ethylene diamine (en), glacial acetic acid, absolute ethanol, $FeCl_3$, $CuSO_4\cdot5H_2O$, $ZnCl_2\cdot H_2O$, $ZrOCl_2\cdot8H_2O$ $K_2Cr_2O_7$, H_2SO_4 and $AgNO_3$ were purchased from Obour Pharmaceutical Industrial Company and Aldrich Chemical Co. All glass were steeped overnight in chromic blend (Potassium dichromate + concentrated sulfuric acid) swill completely with bidistilled water and desiccated in an oven at 100 °C

Preparation of GMFX-en Schiff Base ($C_{38}H_{44}F_2N_{12}O_6$)

An ethanolic solution was formed by combining 30 mL gemifloxacin (2 mmol, 0.77 g) with 40 mL ethylenediamine (1 mmol, 0.07 mL) and refluxing it for 4 h in the existence of 1 mL glacial acetic acid. The subsequent combination was settling on a water bath, and then, the temperature was lowered to 0 °C. Yellowish-white precipitate was collected out, washed multiple spells by way of ethyl alcohol and desiccated below vacuum over $CaCl_2$.

Preparation of Metal Complexes

The dark red $[Fe(GMFX\text{-}en)(H_2O)_2]Cl_3\cdot7H_2O$ complex A was prepared by blending 0.5 mmol (0.401 g) of GMFX-en in 30 mL absolute ethyl alcohol with 0.5 mmol (0.081 g) of $FeCl_3$ in 20 mL ethyl alcohol. The blend was refluxed for 3 h and the subsequent was collected out and desiccated under below vacuum over $CaCl_2$. The brown, light brown, dark brown solid complexes $[Cu(GMFX\text{-}en)(H_2O)_2]SO_4\cdot5H_2O$ complex B, $[Zn(GMFX\text{-}en)(H_2O)_2]Cl_2\cdot3H_2O$ complex C and $[ZrO(GMFX\text{-}en)(H_2O)]Cl_2\cdot5H_2O$ complex D were set in identical technique qualified above by utilizing $CuSO_4\cdot5H_2O$, $ZnCl_2\cdot H_2O$ and $ZrOCl_2\cdot8H_2O$, respectively.

Instruments

The Carbon, Hydrogen and Nitrogen were done elemental experiments done via a Perkin Elmer 2400 CHN elemental analyzer. The proportion of metal ions was gravimetrically measured by transforming solid compounds into metal oxide and using the atomic

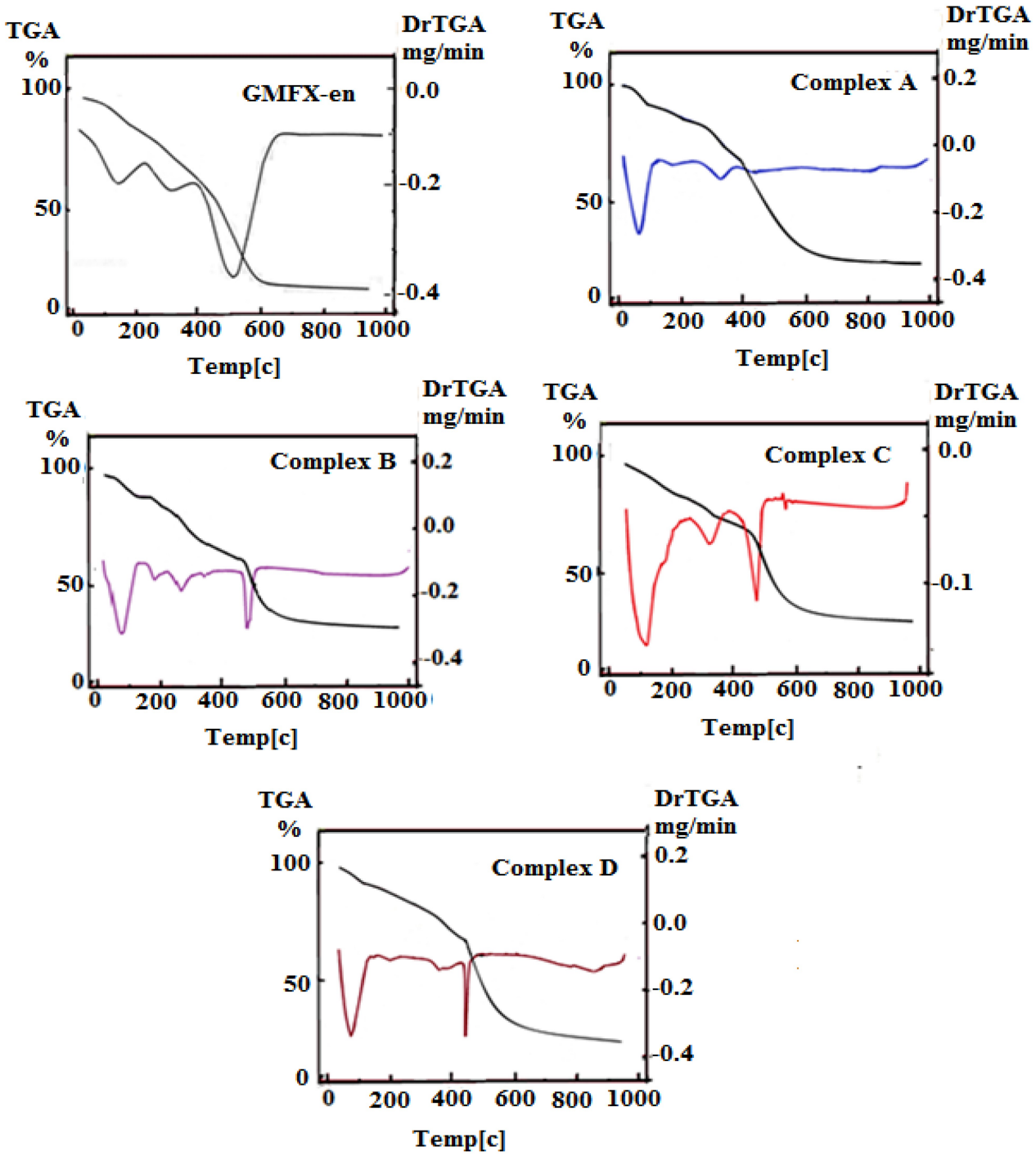

Figure 5. TGA and DTG diagram for GMFX-en and its metal complexes.

absorption technique utilizing a spectrometer model PYE-UNICAM SP 1900 fitted with the corresponding lamp. FT-IR spectra in KBr discs were enrolled in the area from 4000–400 cm^{-1} with FT-IR 460 PLUS Spectrophotometer.^{1}H-NMR spectra have been registered on Varian Mercury VX-300 NMR Spectrometer utilizing (D_6)DMSO as solvent. TG-DTG processes were conducted out under N_2 atmospheric conditions within the temperature range from ambient temperature to 1000 °C using TGA-50H Shimadzu, the sample weight was precisely weighted in an aluminum crucible. The absorption spectra were registered as solutions in (D_6)

Table 5. Thermal behavior and kinetic parameters determined using Coats-Redfern (CR) and Horowitz-Metzger (HM) operated for GMFX-en and its metal complexes.

Compound	Decomposition Range (K)	T_s (K)	Method	Parameters					$R^{[a]}$	$SD^{[b]}$
				E* (KJ/mol)	A (s^{-1})	ΔS* (KJ/mol.K)	ΔH* (KJ/mol)	ΔG* (KJ/mol)		
GMFX-en	318–524	448	CR	76.43	2.42×10^{9}	−0.0686	72.70	103.44	0.965	0.208
			HM	87.35	1.33×10^{8}	−0.0927	83.62	125.16	0.958	0.227
	524–687	623	CR	142.64	1.08×10^{13}	−0.0014	137.46	138.37	0.964	0.212
			HM	170.89	1.88×10^{12}	−0.0160	165.71	175.71	0.959	0.227
	690–973	810	CR	134.71	1.73×10^{6}	−0.1337	127.98	235.31	0.972	0.252
			HM	141.87	1.88×10^{6}	−0.1233	135.14	235.03	0.964	0.289
Complex A	287–405	342	CR	62.07	2.17×10^{9}	−0.0673	59.23	82.25	0.971	0.184
			HM	61.44	2.55×10^{7}	−0.1042	58.60	94.25	0.962	0.202
Complex B	287–411	351	CR	76.53	4.58×10^{8}	−0.0476	79.38	96.11	0.974	0.168
			HM	82.30	2.36×10^{10}	−0.0804	73.61	101.85	0.978	0.155
	709–1273	762	CR	229.49	4.27×10^{13}	0.0082	223.16	216.88	0.991	0.107
			HM	253.54	1.23×10^{18}	0.0936	247.20	175.87	0.984	0.192
Complex C	309–389	366	CR	70.39	2.91×10^{6}	−0.12285	67.34	112.31	0.974	0.171
			HM	78.70	2.00×10^{9}	−0.06852	75.66	100.74	0.969	0.186
	628–830	744	CR	112.49	1.16×10^{8}	−0.0980	106.30	179.27	0.954	0.342
			HM	181.18	3.43×10^{10}	−0.0508	174.99	168.81	0.950	0.263
Complex D	304–398	351	CR	70.39	3.16×10^{6}	−0.1218	67.47	110.22	0.974	0.171
			HM	72.38	6.97×10^{8}	−0.0769	69.46	96.48	0.969	0.186
	654–1273	740	CR	243.17	5.22×10^{16}	0.06757	237.01	187.01	0.996	0.087
			HM	296.47	9.16×10^{18}	0.11052	290.32	208.53	0.995	0.100

[a] correlation coefficients of the Arrhenius plots and [b] standard deviation.

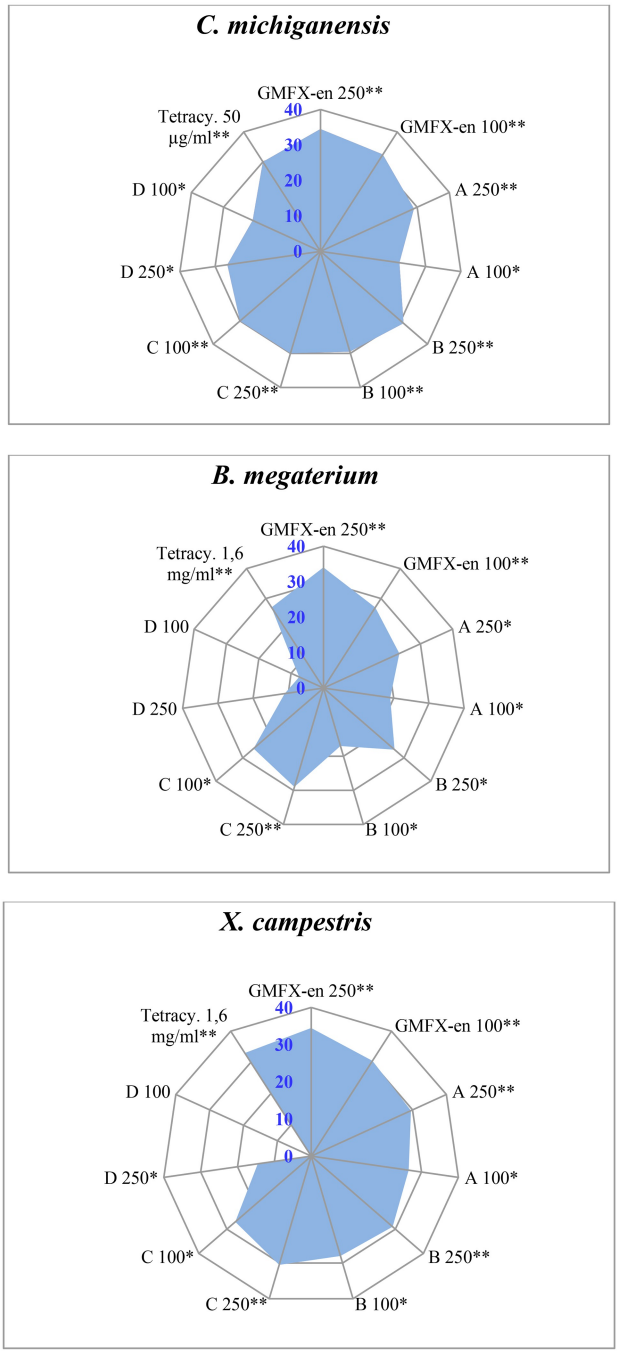

Figure 6. Antibacterial activities of GMFX-en and its metal complexes. Values are recorded as the mean of diameter of inhibition zones (mm) from three replicates ± SDs. (*): statistically significant according to *Tukey* B test at $P < 0.05$: (**): statistically significant at $P < 0.01$. Where A = Complex A, B = complex B, C = complex C, D = complex D and Tetracy.: Tetracycline at 1.6 mg/mL.

DMSO. Room temperature magnetic susceptibility of the powdered samples was applied to the scientific magnetic balance of Sherwood utilizing Gouy at room temperature employing $Hg[Co(CSN)_4]$ as a calibrant. Melting points have been transcribed on the Büchi apparatus. All tests were done with freshly formulated solutions at room temperature. The molar conductivity of the ligand solutions and their complexes at 1×10^{-3} M in dimethylformamide was registered at room temperature using CONSORT K410.

Antimicrobial Investigation

Antibacterial Activity Assay

Tested bacteria. The tested bacterial strains were *C. michiganensis*, *X. campestris* and *B. megaterium* and have been conserved as pure cultures in the collection of the School of Agricultural, Forestry, Food and Environmental Sciences (SAFE), University of Basilicata, Potenza, Italy.

Bactericidal assay. The method of disc diffusion was executed.[56] Every strain's bacterial suspension was made in sterile Millipore H_2O, then inserted into soft agar (0.7 %) and regulated by UV-spectrophotometer (DAS s.r.l., Rome, Italy) to 10^8 colony form units per milliliter (CFU/mL). In a Petri dish (Φ 9 cm) filled with 10 mL of king B nutrient media (KB), 4 mL of each tested bacterial suspension (10 %) was poured. Blank Discs (6 mm) (OXOID, Milan, Italy) were mounted on KB Petri and 20 µL of each suspension was transferred at concentrations: 100 and 250 ppm. Tetracycline (160 µg/mL) was utilized as control. The antimicrobial effect was determined after 24 h at 37 °C, by measuring the diameter of inhibition zones (mm). The experiment was carried out in triplicate with ± SDs.

Antifungal Activity Assay

Tested fungi. The tested phytopathogenic fungi were *M. fructicola*, *P. digitatum* and *C. acutatum*. All tested fungi were cultured on potato dextrose agar (PDA) and were previously identified using morphological and molecular methods. The amplicons were sequenced right away and matched to those in GenBank using Simple Local Alignment Search Tool program from 1990 (BLAST, USA). They were stored at 4 °C as pure cultures in the mycotheca of SAFE, University of Basilicata, Potenza, Italy.

Fungicidal assay. The fungicidal effectiveness of the studied compounds was determined by using incorporation assay,[57] into PDA medium at two concentrations (50 and 100 ppm). Every Petri dish was inocu-

Table 6. Antifungal activity of GMFX-en and its metal complexes.

Compounds	PPM	Fungal growth inhibition (%)		
		P. digitatum	*C. acutatum*	*M. fructicola*
GMFX-en	100	72.5 ± 4.1^{b}	62.5 ± 2.8^{b}	65.0 ± 6.2^{b}
	50	28.0 ± 3.5^{c}	22.5 ± 3.7^{d}	36.0 ± 3.1^{c}
Complex A	100	100.0 ± 0.0^{a}	0.0 ± 0.0^{e}	87.5 ± 5.7^{a}
	50	62.5 ± 8.2^{b}	0.0 ± 0.0^{e}	62.5 ± 6.2^{b}
Complex B	100	100.0 ± 0.0^{a}	45.0 ± 2.1^{c}	85.0 ± 1.8^{a}
	50	62.5 ± 6.5^{b}	0.0 ± 0.0^{e}	75.0 ± 5.2^{ab}
Complex C	100	82.5 ± 7.5^{ab}	77.5 ± 6.5^{b}	82.5 ± 5.4^{a}
	50	61.0 ± 2.5^{b}	32.5 ± 4.5^{c}	62.5 ± 4.2^{b}
Complex D	100	86.0 ± 6.1^{ab}	0.0 ± 0.0^{e}	85.0 ± 5.8^{a}
	50	52.0 ± 4.3^{bc}	0.0 ± 0.0^{e}	67.5 ± 2.2^{b}
Cont.	PDA	0.0 ± 0.0^{d}	0.0 ± 0.0^{e}	0.0 ± 0.0^{d}
Azoxy.	+ ve cont.	58.1 ± 1.2b	92.5 ± 1.3a	45.3 ± 2.1^{c}

Values were recorded as the mean inhibition percentage of fungal growth (three replicates) ± SDs. Values followed by different letters in each vertical column were significantly different according to *Tukey* B test at $P < 0.05$. Cont (PDA): potato dextrose agar (negative control). Azoxy.: Azoxystrobin (Positive control at 0.8 μL/mL).

lated with a fungal disk (0.5 cm), from 96 h fresh culture. All plates were incubated at 22 °C for 96 h and the antifungal effect was estimated by measuring the diameter of the fungal mycelium (mm) compared to control (only PDA + Fungi). The percentage of mycelium growth inhibition (MGI) was calculated according to Zygadlo et al.,[58] (Formula 1) compared to Azoxystrobin (0.8 μL/mL):

$$\text{MGI } (\%) = \frac{(GC - GT)}{GC} \times 100 \quad (1)$$

Where MGI is the percentage of mycelium growth inhibition, GC is the average diameter of fungal mycelium in PDA (control), and GT is the average diameter of fungal mycelium on the treated PDA dish.

Phytotoxicity Assay

The potential phytotoxic efficacy of the tested compounds was investigated on tomato and garden cress plants.[59,60] Seeds were sterilized for 1 min in 3% H_2O_2 then were immerged in Millipore H_2O. Seeds were shaken gently for 2 h in dH_2O (control) or the above-mentioned treatments. The tested concentrations were 2000, 1000, 500, 250 and 100 ppm. All seeds were placed in Petri dishes with filter paper (9 cm, Whatman No. 1). Two mL of dH_2O or various compounds was added to each plate then sealed with Parafilm. All Petri dishes were incubated for 4 days in growth chamber at 24 °C and 60% humidity. The radical length was calculated in cm and the germinated seeds were enumerated. The experiment was repeated three times, and the germination index (GI) was measured as following:

$$\text{G.I. } (\%) = \frac{\text{SG.t} \times \text{RE.t}}{\text{SG.c} \times \text{RE.c}} \times 100 \quad (2)$$

All values are expressed as the mean ± SDs. GI: germination index; SG.t: average germination (Treated seeds); RE.t: average radical elongation (treated seeds); SG.c: average germination (control); RE.c: average radical elongation (control). The statistical analysis was performed using SPSS software with post hoc *Tukey* B ($P < 0.05$).

Data Availability Statement

The data that support the findings of this study are available from the corresponding author upon reasonable request.

Acknowledgments

The authors gratefully acknowledge Zagazig University, Egypt for the support of this research work.

Author Contribution Statement

A.A. Mohamed: Methodology, Formal analysis, Data curation, Investigation. Writing – review & editing. H.S. Elshafie: Methodology, Formal analysis, Investigation, Data curation, Writing – review & editing. S.A. Sadeek: Data curation, Writing – review& editing, Supervision. I. Camele: Data curation, Writing – review & editing, Supervision.

References

[1] M. d. Abu Saleh, Md. Solayman, M. M. Hoque, M. A. K. Khan, M. G. Sarwar, M. A. Halim, 'Inhibition of DNA Topoisomerase Type IIα (TOP2 A) by Mitoxantrone and Its Halogenated Derivatives: A Combined Density Functional and Molecular Docking Study', *Biomed. Res.* **2016**, *2016*, 1–12.

[2] Q. Shi, L. Xu, J. Ji, Y. Li, R. Wang, Z. Zhou, R. Cao, 'Syntheses and structures of two anion-templated dinuclear cadmium complexes with diamino-binaphthyl Schiff bases as ligands', *Inorg. Chem. Commun.* **2004**, *7*, 1254–1257.

[3] W. M. Al-Adiwish, W. A. Yaacob, D. Adan, I. Nazlina, 'Synthesis and Antibacterial Activity of Thiophenes', *Int. J. Adv. Sci. Eng. Inf. Technol.* **2012**, *2*, 27–30.

[4] H. N. Aliyu, R. S. Zayyan, 'Synthesis, Analysis and Bioactivity Evaluation of Copper(II) Tetradentate Schiff Base Complex', *Int. J. Curr. Microbiol. App. Sci.* **2014**, *3*, 445–452.

[5] N. Al-Shaalan, 'Characterization and Biological Activities of Cu(II), Co(II), Mn(II), Fe(II), and UO_2(VI) Complexes with a New Schiff Base Hydrazone: *O*-Hydroxyacetophenone-7-chloro-4-quinoline Hydrazone', *Molecules* **2011**, *16*, 8629–8645.

[6] M. Shebl, S. M. E. Khalil, S. A. Ahmed, H. A. A. Medien, 'Synthesis, spectroscopic characterization and antimicrobial activity of mono-, bi- and tri-nuclear metal complexes of a new Schiff base ligand', *J. Mol. Struct.* **2010**, *980*, 39–50.

[7] K. Ahmad, A. H. Shah, B. Adhikari, U. A. Rana, S. Noman uddin, C. Vijayaratnam, N. Muhammad, S. Shujah, A. Rauf, H. Hussain, A. Badshah, R. Qureshi, H. B. Kraatz and A. Shah, 'pH-dependent redox mechanism and evaluation of kinetic and thermodynamic parameters of a novel anthraquinone', *RSC Adv.* **2014**, *4*, 31657–31665.

[8] A. K. Alam, A. S. Hossain, M. A. Khan, S. R. Kabir, Md. A. Reza, Md. M. Rahman, M. S. Islam, Md. A. Abdur Rahman, M. Rashid, Md. G. Sadik, 'The Antioxidative Fraction of White Mulberry Induces Apoptosis through Regulation of p53 and NFκB in EAC Cells', *PLoS One* **2016**, *11*, e0167536.

[9] S. A. Sadeek, S. M. Abd El-Hamid, M. M. El-Aasser, 'Synthesis, characterization, antimicrobial and cytotoxicity studies of some transition metal complexes with gemifloxacin', *Monatsh. Chem.* **2015**, *146*, 1967–1982.

[10] O. Yukako, 'Excitation Energy Dependence of Transient Absorptions of [N, N′-o Phenylenebis (salicylideneaminato)] cobalt(II) in Dmf Solution', *Bull. Chem. Soc. Jpn.* **1997**, *70*, 1319–1324.

[11] W. H. Elshwiniy, A. G. Ibrahim, S. A. Sadeek, W. A. Zordok, 'Ligational, density functional theory and biological studies on some new Schiff base 2-(2 hydroxyphenylimine)benzoic acid (L) metal complexes', *Appl. Organomet. Chem.* **2020**, *34*, e5819.

[12] W. H. Elshwiniy, A. G. Ibrahim, S. A. Sadeek, W. A. Zordok, 'Synthesis, structural elucidation, molecular modeling and antimicrobial studies of 6-(2-hydroxyphenylimine)-2-thioxotetrahydropyrimidin-4(1H)-one (L) Schiff base metal complexes', *Appl. Organomet. Chem.* **2021**, *35*, e6174.

[13] S. A. Sadeek, M. S. El-Attar, S. M. Abd El-Hamid, 'Synthesis and characterization and antibacterial activity of some new transition metal complexes with ciprofloxacin-imine', *Bull. Chem. Soc. Ethiop.* **2015**, *29*, 259–274.

[14] D. M. Johnson, R. N. Jones, M. E. Erwin, 'Anti-streptococcal activity of SB-265805 (LB20304), a novel fluoronaphthyridone, compared with five other compounds, including quality control guidelines', *Diagn. Microbiol. Infect. Dis.* **1999**, *33*, 87–91..

[15] R. Grossman, J. Rotschafer, J. S. Tan, 'Antimicrobial treatment of lower respiratory tract infections in the hospital setting', *Am. J. Med.* **2005**, *118*, 29–38.

[16] S. A. Sadeek, S. M. Abd El-Hamid, W. H. El-Shwiniy, 'Synthesis, spectroscopic characterization, thermal stability and biological studies of mixed ligand complexes of gemifloxacin drug and 2, 2′-bipyridine with some transition metals', *Res. Chem. Intermed.* **2016**, *42*, 3183–3208.

[17] A. Vitti, H. S. Elshafie, G. Logozzo, S. Marzario, A. Scopa, I. Camele, M. Nuzzaci, 'Physico-chemical characterization and biological activities of a digestate and a more stabilized digestate-derived compost from agro-waste', *Plants* **2021**, *10*, 386.

[18] W. H. El-Shwiniy, W. S. Shehab, S. F. Mohamed, H. G. Ibrahium, 'Synthesis and cytotoxic evaluation of some substituted pyrazole zirconium (IV) complexes and their biological assay', *Appl. Organomet. Chem.* **2018**, *32*, e4503.

[19] F. M. Ahmed, S. A. Sadeek, W. H. El-Shwiniy, 'Synthesis, Spectroscopic Studies, and Biological Activity of Some New N_2O_2 Tetradentate Schiff Base Metal Complexes', *Russ. J. Gen. Chem.* **2019**, *89*, 1874–1883.

[20] M. A. Gamil, S. A. Sadeek, W. A. Zordok, W. H. El-Shwiniy, 'Spectroscopic, DFT modeling and biological study of some new mixed ligand metal complexes derived from gatifloxacin and pregabalin', *J. Mol. Struct.* **2020**, *1209*, 127641.

[21] S. M. Abd El-Hamid, S. A. Sadeek, W. A. Zordok, W. H. El-Shwiniy, 'Synthesis, spectroscopic studies, DFT calculations, cytotoxicity and antimicrobial activity of some metal complexes with ofloxacin and 2,2′-bipyridine', *J. Mol. Struct.* **2019**, *1176*, 422–433.

[22] G. Pasomas, A. Tarushi, E. K. Efthimiadou, 'Synthesis, characterization and DNA-binding of the mononuclear dioxouranium(VI) complex with ciprofloxacin', *Polyhedron* **2008**, *27*, 133–138.

[23] G. Kumar, S. Devi, R. Johari, D. Kumar, 'Evaluation of Ecotoxicology Assessment Methods of Nanomaterials and Their Effects', *Eur. J. Med. Chem.* **2012**, *52*, 269–274.

[24] O. A. El-Gammal, S. A. El-Brashy, G. M. Abu El-Reash, 'Macrocyclic Cr^{3+}, Mn^{2+} and Fe^{3+} complexes of a mimic SOD moiety: Design, structural aspects, DFT, XRD, optical properties and biological activity', *Appl. Organomet. Chem.* **2020**, *34*, e5456.

[25] A. B. P. Lever, '*Inorganic Electronic Spectroscopy*', Amsterdam, **1963**.

[26] B. N. Figgis, M. A. Hitchman, '*Applications*', Wiley-VCH, New York, **2000**.
[27] S. Defazio, R. Cini, 'Synthesis, X-ray structure and molecular modeling analysis of cobalt(II), nickel(II), zinc(II) and cadmium(II) complexes of the widely used anti-inflammatory drug_meloxicam', *J. Chem. Soc. Dalton Trans.* **2002**, *22*, 1888-. 1897.
[28] S. A. Sadeek, 'Synthesis, thermogravimetric analysis, infrared, electronic and mass spectra of Mn(II), Co(II) and Fe(III) norfloxacin complexes', *J. Mol. Struct.* **2005**, *753*, 1–12.
[29] M. F. Hochella, '19-Carbon nanotubes: An efficient sorbent for herbicide sensing and remediation', *J. Nanosci. Nanotechnol.* **2002**, *203*, 593–605.
[30] W. H. Mahmoud, R. G. Deghadi, G. G. Mohamed, 'Metal complexes of ferrocenyl-substituted Schiff base: Preparation, characterization, molecular structure, molecular docking studies, and biological investigation', *J. Organomet. Chem.* **2020**, *917*, 121113.
[31] S. A. Sadeek and W. H. EL-Shwiniy, 'Metal complexes of the third generation quinolone antibacterial drug sparfloxacin: preparation, structure, and microbial evaluation', *J. Coord. Chem.* **2010**, *63*, 3471–3482.
[32] A. A. Mohamed, S. A. Sadeek, S. M. Abd El-Hamid, W. A. Zordok, H. M. Awad, 'Mixed-ligand complexes of tenoxicam drug with some transition metal ions in presence of 2,2′-bipyridine: Synthesis, spectroscopic characterization, thermal analysis, density functional theory and in vitro cytotoxic activity', *J. Mol. Struct.* **2019**, *1197*, 628–644.
[33] S. A. Sadeek, A. A. Mohamed, H. A. El-Sayed, M. S. El-Attar, 'Spectroscopic characterization, thermogravimetric and antimicrobial studies of some new metal complexes derived from4-(4-Isopropyl phenyl)-2-oxo-6-phenyl 1, 2-dihyropyridine-3-carbonitrile (L)', *Appl. Organomet. Chem.* **2019**, *34*, e5334.
[34] L. J. Bellamy, '*The Infrared Spectra of Complex Molecules*, third ed., Chapman and Hall', London, **1975**.
[35] F. A. Cotton, G. Wilkinson, C. A. Murillo, M. Bochmann, '*Adv. Inorg. Chem.* 6th ed., Wiley', New York, **1999**, *1054*.
[36] A. Tavman, 'Synthesis, spectral characterisation of 2-(5-methyl-1*H*-benzimidazol-2-yl)-4-bromo/nitro-phenols and their complexes with zinc(II) ion, and solvent effect on complexation', *Spectrochim. Acta Part A* **2006**, *63*, 343–348.
[37] S. M. Ben-Saber, A. A. Maihub, S. S. Hudere, M. M. El-ajaily, 'Complexation behavior of Schiff base toward transition metal ions', *Microchem. J.* **2005**, *81*, 191–194..
[38] P. Anant, K. S. Bibhesh, B. Narendar, 'Synthesis and Characterization of Luminescent Zinc(II) and Cadmium(II) Complexes with N,S-Chelating Schiff Base Ligands', *Spectrochim. Acta Part A* **2010**, *76*, 356–362.
[39] M. Saif, M. M. Mashaly, M. F. Eid, R. Fouad, 'characterization and thermal studies of binary and/or mixed ligand complexes of Cd(II), Cu(II), Ni(II) and Co(III) based on 2-(Hydroxybenzylidene) thiosemicarbazone: DNA binding affinity of binary Cu(II) complex', *Spectrochim. Acta Part A.* **2012**, *92*, 347.
[40] S. A. Sadeek, S. M. Abd El-Hamid, N. G. Rashid, 'Spectroscopic Characterization and XRD of Some New Metal Complexes with Dithranol in Presence of 8-hydroxyquinoline', *Egypt. J. Chem.* **2020**, *3*, 939–951.
[41] S. A. Sadeek, W. H. EL-Shwiniy, W. A. Zordok, A. M. EL-Didamony, 'Spectroscopic, structure ad antimicrobial activity of new Y(III) and Zr(IV) ciprofloxacin', *Spectrochim. Acta Part A* **2011**, *78*, 854–867.
[42] A. W. Coats, J. P. Redfern, 'Kinetic parameters from thermogravimetric data', *Nature* **1964**, *201*, 68–69.
[43] H. W. Horowitz, G. Metzger, 'A new analysis of thermogravimetric traces', *Anal. Chem.* **1963**, *35*, 1464–1468.
[44] A. A. Frost, R. G. Pearson, '*Kinetics and Mechanism*', Wiley, New York. **1961**.
[45] S. Ilhan, H. Temel, I. Yilmaz, A. Kilic, 'Synthesis, characterization and redox properties of macrocyclic Schiff base by reaction of 2, 6-diaminopyridine and 1, 3-*bis*(2-carboxyaldehyde phenoxy)propane and its Cu^{II}, Ni^{II}, Pb^{II}, Co^{III} and La^{III} complexes', *Transition Met. Chem.* **2007**, *32*, 344–349.
[46] O. A. El-Gammal, M. M. Bekheit, S. A. El-Brashy, 'Synthesis, characterization and *In Vitro* antimicrobial studies of Co(II), Ni(II) and Cu(II) complexes derived from macrocyclic compartmental ligand', *Spectrochim. Acta Part A* **2015**, *137*, 207–219.
[47] T. Hatakeyama, F. X. Quinn, '*Thermal Analysis Fundamentals and Applications to Polymer Science*', 2nd ed., Wiley, Chichester. **1994**.
[48] H. S. Elshafie, S. A. Sadeek, I. Camele, A. A. Mohamed, 'Biological and Spectroscopic Investigations of New Tenoxicam and 1. 10-Phenthroline Metal Complexes', *Molecules* **2020**, *25*, 1027.
[49] S. H. Sakr, H. S. Elshafie, I. Camele, S. A. Sadeek, 'Synthesis, spectroscopic, and biological studies of mixed ligand complexes of gemifloxacin and glycine with Zn (II), Sn (II), and Ce (III)', *Molecules* **2018**, *23*, 1182.
[50] H. S. Elshafie, L. Viggiani, M. S. Mostafa, M. A. El-Hashash, S. A. Bufo, I. Camele, 'Biological activity and chemical identification of ornithine lipid produced by Burkholderia gladioli pv. agaricicola ICMP 11096 using LC/MS and NMR analyses', *J. Biol. Res.* **2017**, *90*, 96–103.
[51] I. Camele, H. S. Elshafie, V. De Feo, L. Caputo, 'Anti-quorum sensing and antimicrobial effect of Mediterranean plant essential oils against phytopathogenic bacteria', *Front. Microbiol.* **2019**, *10*, 2619.
[52] N. H. Patel, H. M. Parekh, M. N. Patel, 'Synthesis, physicochemical characteristics, and biocidal activity of some transition metal mixed-ligand complexes with bidentate (NO and NN) Schiff bases', *Pharm. Chem. J.* **2007**, *1*, 78–81.
[53] H. S. Elshafie, M. Amato, V. De Feo, I. Camele, 'Chemical composition and antimicrobial activity of Chia (*Salvia hispanica* l.) essential oil', *Eur. Food Res. Technol.* **2018**, *244*, 1675–1682.
[54] H. S. Elshafie, L. Caputo, L. De Martino, D. Gruľová, V. D. Zheljazkov, V. De Feo, I. Camele, 'Biological investigations of essential oils extracted from three *Juniperus* species and evaluation of their antimicrobial, antioxidant and cytotoxic activities', *J. Appl. Microbiol.* **2020**, *129*, 1261–1271.
[55] H. S. Elshafie, I. Camele, A. Sofo, G. Mazzone, M. Caivano, S. Masi, D. Caniani, 'Mycoremediation effect of *Trichoderma harzianum* strain T22 combined with ozonation in diesel-contaminted sand', *Chemosphere* **2020**, *252*, 126597.
[56] H. S. Elshafie, E. Mancini, I. Camele, L. De Martino, V. De Feo, 'In vivo antifungal activity of two essential oils from Mediterranean plants against postharvest brown rot disease of peach fruit', *Ind. Crops Prod.* **2015**, *66*, 11–15.
[57] H. S. Elshafie, S. H. Sakr, S. A. Sadeek, I. Camele, 'Biological investigations and spectroscopic studies of new Moxiflox-

acin/Glycine-Metal complexes', *Chem. Biodiversity* **2019**, *16*, e1800633.
[58] J. A. Zygadlo, C. A. Guzman, N. R. Grosso, 'Antifungal properties of the leaf oils of Tagetes minuta L. and T. filifolia Lag', *J. Essent. Oil Res.* **1994**, *6*, 617–621.
[59] F. Ceglie, H. S. Elshafie, V. Verrastro, F. Tittarelli, 'Evaluation of Olive Pomace and Green Waste Composts as Peat Substitutes for Organic Tomato Seedling Production', *Compost Sci. Util.* **2011**, *19*, 293–300..
[60] E. Fallik, J. Klein, S. Grinberg, E. Lomaniee, S. Lurie, A. Lalazar, 'Effect of postharvest heat treatment of tomatoes on fruit ripening and decay caused by Botrytis cinerea', *Plant Dis.* **1993**, *77*, 985–988.

Received May 12, 2021
Accepted June 29, 2021

